16TH EUROPEAN CONFERENCE ON EARTHQUAKE ENGINEERING THESSALONIKI 18 - 21 JUNE 2018

CONSIDERATIONS FOR THE SEISMIC DESIGN CODE OF UNDERGROUND STRUCTURES IN CHINA

Jian-Min ZHANG[1], Rui WANG[2]

ABSTRACT

Underground structure construction in China has experienced an astonishing growth during the past decade, with the number of cities with subways increasing from 12 in 2007 to well over 30 in 2017. The boom in underground structure construction has created new challenges and demands for the seismic design of underground structures in China, for which a specifically dedicated seismic design code has not been published until now. This paper discusses some key concepts and methods taken into consideration in the development of the Chinese code for seismic design of underground structures. The seismic response and demand computation methods for various underground structures in different site types are clearly designated, with special considerations given for underground structures in liquefiable sites. Seismic performance levels are assigned for underground structures of different importance, and limiting values for seismic induced underground structure deformation is evaluated. The effects of soil profile are especially considered, promoting the use of high fidelity methods to determine the seismic response of soil surrounding underground structures. The influence of the existence of underground structures on the liquefaction of surrounding soil is determined, adopting a liquefaction assessment method that takes underground structures into consideration. The upheaval induced by soil liquefaction is checked against.

Keywords: Underground structure; Seismic design; Structure deformation; Soil profile; Liquefaction

1. INTRODUCTION

The past decade has witnessed an astonishing growth in underground structure construction during the past decade, with the number of cities with subways increasing from 12 in 2007 to well over 30 in 2017. The boom in underground structure construction has created new challenges and demands for the seismic design of underground structures in China. Increasing number of underground structures are under construction in China in seismically active areas with complicated soil conditions. For example, the subway lines and stations in Xuzhou and Nanjing cut through areas of liquefaction prone saturated sand and silty sand. Severe underground structure damage in liquefiable ground has been reported in past major earthquakes, including the 1995 Kobe earthquake (Samata et al., 1997; Uenishi and Sakurai, 2000) and the 2011 Tohoku earthquake (Tokimatsu et al., 2012; Yasuda et al., 2012; Yamaguchi et al., 2012), suggesting that underground structures in liquefiable ground may be vulnerable to seismic damage. However, until now, there is not a seismic design code in China specifically targeting underground structures, which has distinctly different requirements compared to ground structures due to soil-structure interaction.

This paper presents some of the key concepts and methods taken into consideration in the development of the new Chinese Code for the Seismic Design of Underground Structures (CCSDUS).

[1]Professor, Department of Hydraulic Engineering, School of Civil Engineering, National Engineering Laboratory for Green & Safe Construction Technology in Urban Rail Transit, Tsinghua University, Beijing, China, zhangjm@tsinghua.edu.cn

[2]Assistant researcher, Department of Hydraulic Engineering, School of Civil Engineering, National Engineering Laboratory for Green & Safe Construction Technology in Urban Rail Transit, Tsinghua University, Beijing, China, wangrui_05@tsinghua.edu.cn

The performance levels for underground structures of various importance are designated, while the limiting structure deformation values for the different targets are evaluated and presented in Section 2. The importance of accurate soil profiling and use of high fidelity methods in determining the seismic response of underground structures is presented in Section 3, with analysis of an underground structure in three different soil profiles. The influence of the existence of underground structures on the liquefaction of surrounding soil is determined in Section 4. While the method for analyzing the upheaval induced by soil liquefaction is briefly discussed in Section 5.

2. SEISMIC PERFORMANCE LEVELS

The seismic performance requirements of underground structures depends on both the importance of the structure and the ground motion. Underground structures of three categories of importance and under four levels of ground motion are designated to the following four levels of seismic performance levels: I. no damage occurs in the main structure, and the structure is within the linear elastic response stage; II. light damage may occur, which can be repaired rapidly to restore normal functionality, and the structure is within the nonlinear elastic response stage; III. reparable damage may occur, and the structure should be within elasto-plastic stage; IV. no collapse should occur.

The drift ratio of underground structures is a key parameter that can be used to evaluate its seismic performance. The drift ratio is the differential lateral displacement of the top and bottom of the underground structure divided by the height of the structure. The Chinese Code for Seismic Design of Buildings (CCSDB) suggests the limiting values of seismic drift ratio based on those of ground structures. In order to provide appropriate limiting values for the seismic drift ratio of underground structures, pushover analyses are conducted on typical underground structures in Figure 1 embedded in soil. The pushover analysis are conducted using models that consist of both structure and surrounding soil with different modulus.

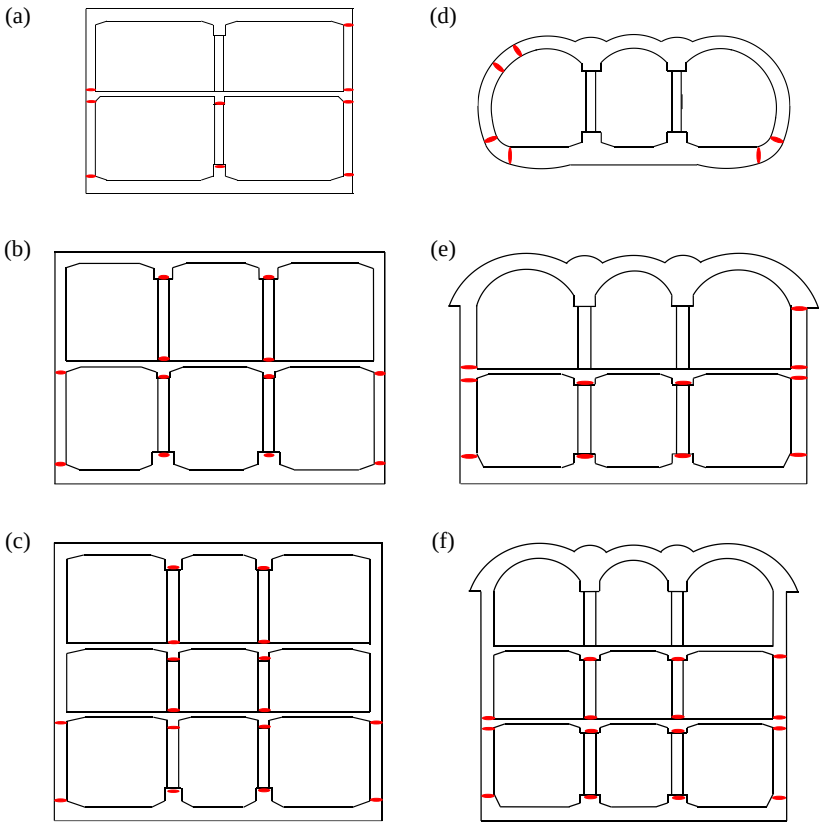

Figure 1. Typical underground structures and the plastic hinges developed in pushover analysis

The plastic hinges that is developed in the structures in the pushover analyses are shown in Figure 1. Most of the plastic hinges appear at the top and bottom of the side walls and central pillars. The drift ratio at which the first plastic hinge appears can be used as the elastic limiting value of the drift value, and the drift ratio at which the structure becomes indeterminate should be used as the elasto-plastic limiting value. Table 1 lists the elastic and elasto-plastic drift ratio limiting values of the six different structures in Figure 1. Based on these analysis and other evidence, the elastic drift ratio limit for underground structures of two stories or less is set to 0.18%, and the elastic drift ratio limit for underground structures of three stories or more is set to 0.1%. The elasto-plastic drift ratio limit for underground structures is set to 0.4%, keeping consistent with the regulation in the CCSDB.

Table 1. List of elastic and elasto-plastic drift ratios.

	Structure (a)				**Structure (d)**					
	elastic		elastio-plastic		elastic			elastio-plastic		
	2m	4m	2m	4m	5m	10m	15m	5m	10m	15m
10	0.61%	0.68%	0.96%	1.07%	0.80%	0.67%	0.59%	1.88%	2.15%	2.69%
E_d/Mpa 150	0.35%	0.29%	1.27%	1.23%	0.60%	0.48%	0.33%	1.39%	0.99%	0.67%
300	0.30%	0.27%	1.01%	0.93%	0.44%	0.43%	0.33%	1.07%	0.83%	0.70%
	Structure (b)				**Structure (e)**					
	elastic		elastio-plastic		elastic			elastio-plastic		
	2m	4m	2m	4m	5m	10m	15m	5m	10m	15m
10	0.37%	0.51%	2.94%	4.09%	0.88%	1.03%	1.33%	2.55%	3.01%	3.94%
E_d/Mpa 150	0.34%	0.61%	1.55%	1.16%	0.36%	0.28%	0.23%	1.17%	1.06%	1.12%
300	0.33%	0.60%	1.23%	1.17%	0.29%	0.25%	0.22%	0.94%	0.85%	0.77%
	Structure (c)				**Structure (f)**					
	elastic		elastio-plastic		elastic			elastio-plastic		
	2m	4m	2m	4m	5m	10m	15m	5m	10m	15m
10	0.96%	0.96%	3.05%	3.12%	1.36%	2.49%	8.55%	4.90%	9.97%	25.04%
E_d/Mpa 150	0.30%	0.27%	1.12%	1.07%	0.28%	0.21%	0.16%	1.29%	1.39%	0.71%
300	0.26%	0.25%	0.88%	0.80%	0.24%	0.20%	0.16%	0.91%	0.88%	0.66%

3. INFLUENCE OF LAYERED SOIL PROFILE

The seismic response of a typical underground structure in three different soil profiles are analyzed in this section, including: (1) underground structure fully embedded in liquefiable soil (Liq, Fig. 2 (a)). (2) liquefiable layer passes through the underground structure (M-liq, Fig. 2 (a)), with the sidewalls in contact with the liquefiable layer, while the top and bottom slabs are in contact with non-liquefiable soil, (3) underground structure in homogeneous non-liquefiable soil (Non-liq, Fig. 2 (a)). The analysis is conducted using solid-fluid coupled FEM simulation via the OpenSees framework using the model shown in Fig. 2 (b). The bottom boundary of the model is constrained to follow the input motion, and is set as an impermeable boundary. Tied displacement degrees of freedom are used at the two lateral boundaries to simulate the free-field motion. The water level is assumed to be at the ground surface, with a free drainage boundary condition. A unified plasticity model for large post-liquefaction shear deformation of sand is used for the liquefiable soil to fully capture the behavior of saturated sand (Wang et al. 2014). A technique of combining beam elements with quadrilateral elements is developed to simulate reinforced concrete structures. The input ground motion is selected based on linear scaled matching of the uniform hazard spectrum (UHS) for Nanjing (Fig. 2 (c)). The initial stress state is setup by first applying the gravity field, followed by excavation of the underground space and placement of the underground structure, adopting the procedures proposed by Wang et al. (2014). Dynamic analysis is then carried out after the initial geo-static step.

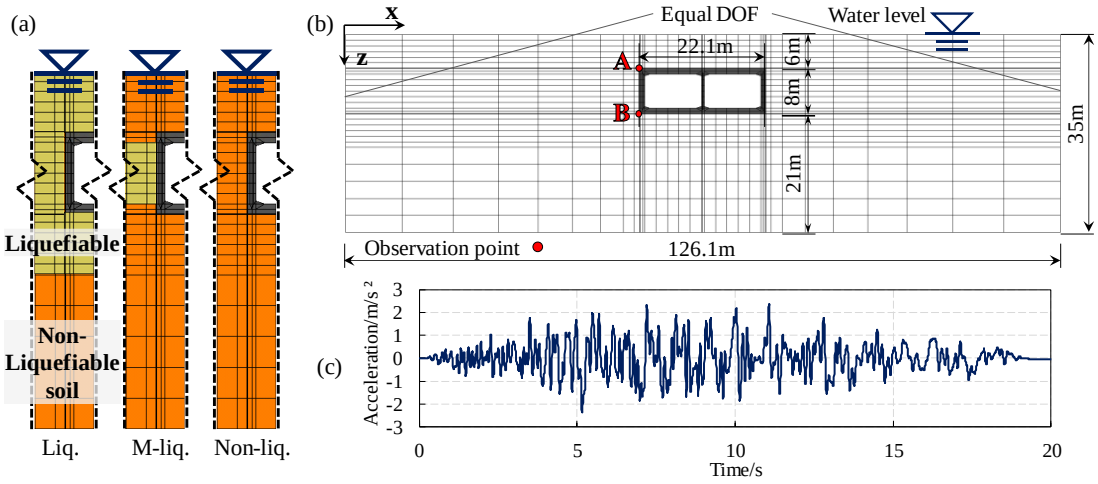

Figure 2. Soil profile, FEM mesh, and input ground motion

Fig. 3 (a) shows dynamic range of the drift ratio in each condition. The maximum drift ratio in the M-liq condition is 120% greater than that in the Non-liq condition, and is 50% greater than that in the Liq condition. Fig. 3 (b) shows the distribution of maximum moments along the left wall and central pillar in the Liq, M-liq, and Non-liq conditions, respectively. The maximum bending moment value occurs at both ends of the walls and pillar. The maximum bending moment at the bottom of the left wall and in both ends of the pillar in the M-liq condition reaches the moment capacity, which could lead to damage of the structure. In the Non-liq condition, the maximum value of bending moment remains well within the moment capacity. In the Liq condition, the maximum bending moment value at the top of the side walls and the pillar are in safe range, but the bending moment at the bottom of the left wall reaches the moment capacity.

Through comparison of structure deformation and internal forces of three different soil profile conditions, the M-liq condition with layered liquefiable soil experiences the greatest drift ratio and bending moments. This suggests that under the same input motion, layered liquefiable soil profile could induce greater structure deformation and internal stress, and is an unfavorable condition compared with underground structures in homogeneous liquefiable soil. Therefore, the CCSDUS requires appropriate methods that can reflect the soil deformation and soil-structure interaction in layered liquefiable ground to be used for the seismic design of underground structures in these conditions.

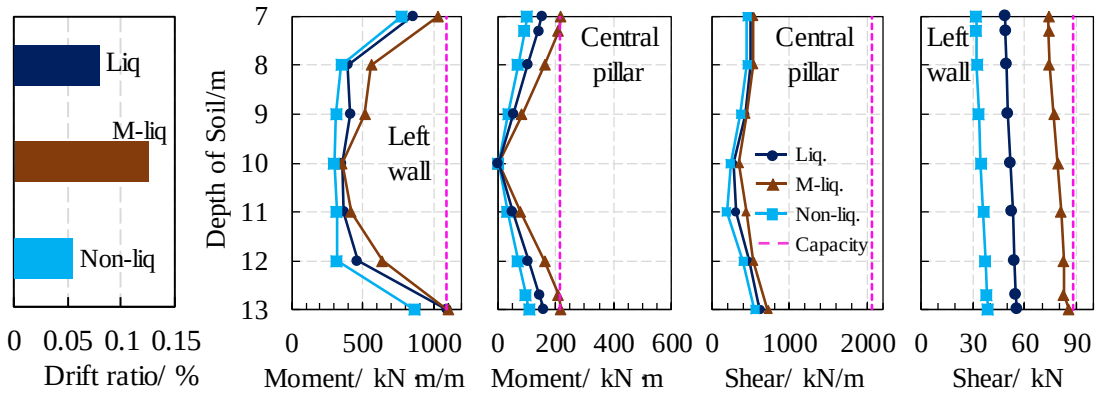

Figure 3. Drift ratio and bending moment of the structure in three different soil profiles

Fig. 4 (a) shows the dynamic range of shear forces on top and bottom slabs of the underground

structure. It is evident that the shear force in the M-liq condition is the greatest, which is at most 40% greater than the Non-liq condition and as much as eight times that of the Liq condition. In the Liq condition, liquefaction takes place under the bottom slab of the structure, which leads to the low stress level with significant shear strain. In the M-liq condition, since no liquefaction takes place on either slab, the increase in shear strain of the liquefied layer would increase the shear force on the structure. The significantly greater shear force acting upon the top and bottom slabs of the underground structure in the M-liq condition compared with that of the other two conditions provides explanation to why the structure response in the M-liq condition is the most intense of the three conditions.

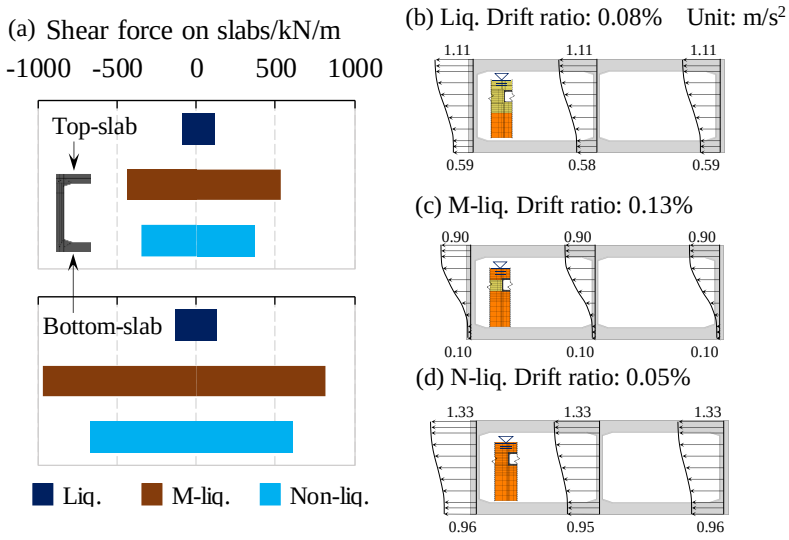

Figure 4. Shear forces and acceleration on the structure in three different soil profiles

However, for the Liq condition, even though the shear force on the top and bottom slabs are smaller than those in the Non-liq condition, its structure response is still more intense than that in the Non-liq condition, which is somewhat counterintuitive. This can be explained through analysis of the inertial force on the underground structure, which is often underappreciated. The acceleration distribution in the structure at the time of maximum drift ratio in each condition is plotted in Fig. 4 (b)-(d). The structure under all the three conditions reaches its maximum drift ratio in the +x direction, being 0.08%, 0.12%, and 0.05% for the Liq, M-liq, and Non-liq conditions, respectively, which means the top slab is at a position relative to the right of the bottom slab. In the Liq and M-liq conditions, the differential acceleration between the top and bottom slab is significant, which is 0.52m/s^2 and 0.80m/s^2, respectively (Fig. 4 (b) (c)). However, in the Non-liq condition, although the absolute value of acceleration is greater than that in the other two conditions, the differential value between the top and bottom slabs is much smaller, at 0.37 m/s^2 (Fig. 4 (d)). This indicates that the loss of constraint from the liquefied soil can lead to greater differential acceleration in the underground structure compared to that of underground structures in non-liquefied soil, which in turn increases the internal forces and deformation of the structure. Unlike existing perception that inertial forces are negligible for underground structures, these results suggest that for underground structures in liquefiable ground, inertial forces can also have a strong impact on seismic response. Thus, the CCSDUS requires inertial forces to be considered in the seismic design of underground structures in liquefiable soil and soft clay.

4. LIQUEFACTION ASSESSMENT CONSIDERING UNDERGROUND STRUCTURE

Underground structures generally have a smaller overall density compared with the soil that they replace, which could thus cause liquefaction to occur at greater depth around the structure. Figure 5 shows the range of liquefied soil under the same seismic input for both a homogeneous saturated sand free field and the same soil with an underground structure embedded, in a numerical simulation. The simulation follows the same method and procedure as that in Section 3. The simulation results show

clearly that the existence of the underground structure causes the liquefaction depth beneath the structure to significantly increase. Extensive study shows that existence of typical underground structures can cause liquefaction depth to extend up to 10m below the structure. However, current codes that mainly target ground structures, such as the Chinese Code for Seismic Design of Buildings does not take the influence of underground structures into consideration during liquefaction assessment, and neglect the liquefaction susceptibility of soil below 20m depth. Although this approach may be appropriate for ground structures which increases the effective stress in the foundation, it could cause fatal underestimation of liquefaction susceptibility for underground structures which decreases the effective stress in the ground. Hence, a new liquefaction assessment method that takes into consideration of underground structures is adopted in the newly developed CCSDUS.

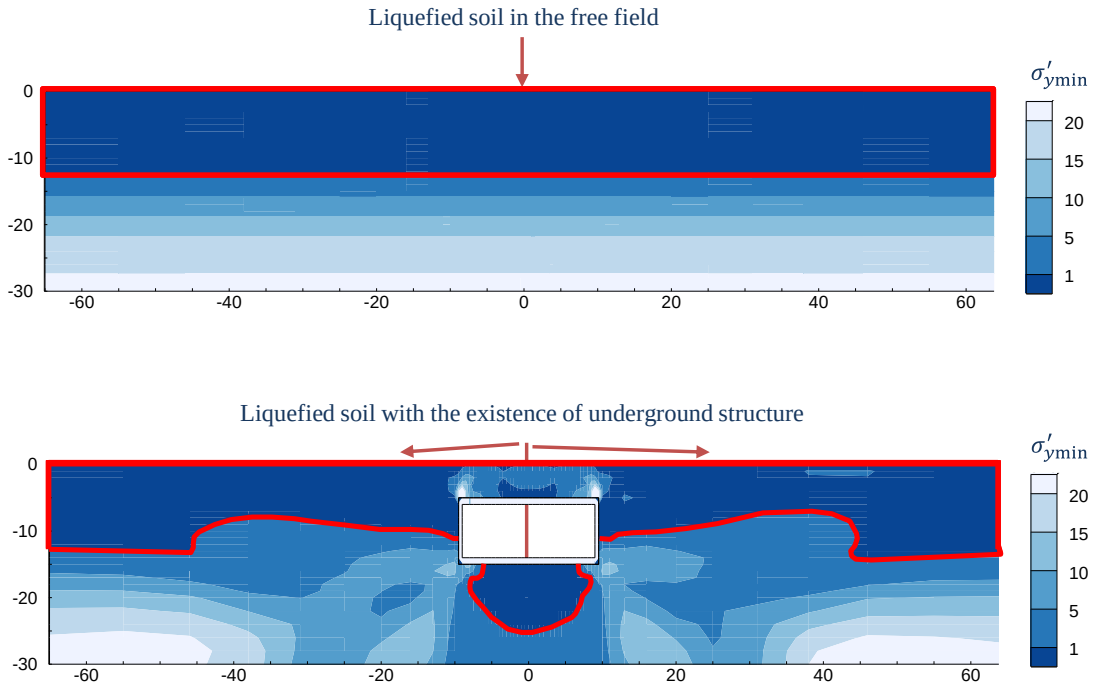

Distribution of minimum vertical effective stress (σ'_{ymin})

Figure 5. Distribution of minimum effective stress during shaking without and with underground structure

When the underground structure is constructed above saturated sand and silty sand, the liquefaction depth D_f obtained from traditional methods that do not take the existence of underground structures into consideration should be modified according to the following equations:

$$D_s = D_f + (1-\eta_{gs})H\xi_s \tag{1}$$

$$\eta_{gs} = \begin{cases} \dfrac{G_{st}}{G_{so}}, & G_{st} < G_{so} \\ 1, & G_{st} \geq G_{so} \end{cases} \tag{2}$$

$$\xi_s = \begin{cases} \dfrac{1.5B}{D_f + H + 0.25B - D} e^{\eta_{gs}}, & D_f > D \\ \dfrac{1.5B}{H + 0.25B} e^{\eta_{gs}}, & D_f \le D \end{cases} \quad (3)$$

Where D_s is the modified liquefaction depth after taking the underground structure into consideration, H , B, and D are the structure height, width, and depth, respectively, η_{gs} is the relative structure density, G_{st} and G_{so} are the structure weight and the corresponding soil weight in the free field, respectively, ξ_s is the structure influence factor. Equations (1)-(3) are developed empirically based on existing experiment and numerical analysis data.

5. UPHEAVAL CAUSED BY LIQUEFACTION

Case studies have shown that the upheaval of underground structures in liquefiable ground is a major cause of failure. In general, underground structures have smaller average densities compared to saturated soil, this upheaval of the underground structure is caused by the increase in excess pore water pressure and the decrease in surrounding soil strength. When the base of the underground structure is within soil that is determined as liquefiable following the procedures in Section 4, the structure should be checked against upheaval, with the requirement that the total uplifting force F should be no greater than the total downward force R_F divided by a safety factor γ_{RF} of 1.05:

$$F \le R_F / \gamma_{RF} \quad (4)$$

The total uplifting force F consists of the uplifting forces generated by the hydro-static pore pressure (F_S) and by the excess pore pressure accumulated during shaking (F_p) (Figure 6), expressed as:

$$F = F_S + F_p \quad (5)$$

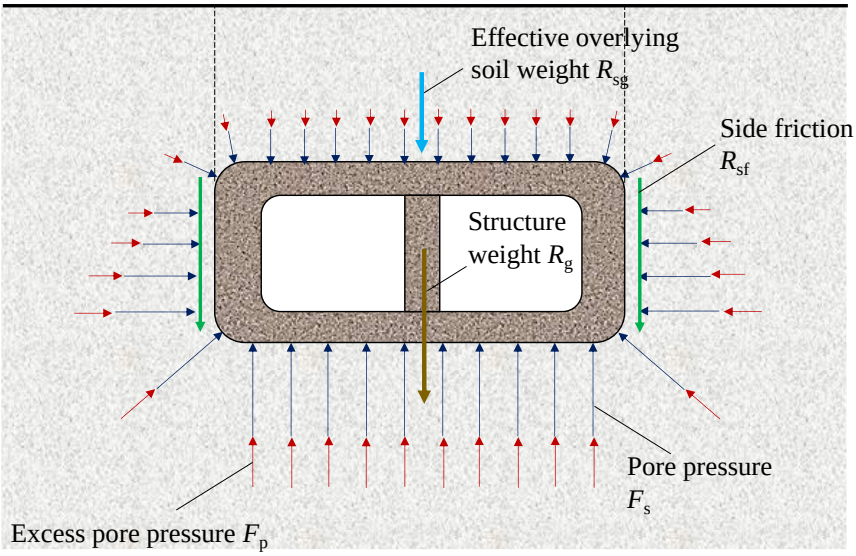

Figure 6. Diagram of uplifting forces and downward forces acting upon underground structures

The excess pore pressure should be obtained through seismic analysis of the soil-structure system. The total resisting downward force R_F consists of the weight of the structure R_g, the effective weight of the overlying soil R_{sg}, and the side friction force R_{sf}:

$$R_F = R_g + R_{sg} + R_{sf} \quad (6)$$

In this formulation the shear strength of the overlying soil is neglected from the resisting downward force, keeping it conservative. In calculating the side friction force R_{sf}, the degradation of the soil friction caused by effective stress decrease should be taken into consideration.

6. CONCLUSIONS

Some of the key considerations for the development of the new Chinese seismic design code for underground structures are presented in this paper. The new code enforces different performance levels for underground structures of various importance. The limiting values of seismic underground structures deformation is analyzed with consideration of surrounding soil, with elastic and elasto-plastic drift ratio limits corresponding to different performance levels. The influence of layered liquefiable deposits on the seismic response of an underground structure is analyzed to highlight the importance of accurate depiction of soil response during seismic design, which promotes the use of high fidelity physical and numerical modelling methods to determine the seismic response of soil surrounding underground structures. Compared with the free field, the existence of underground structures can lead to decreased effective stress and increase in shear effects, resulting in larger bodies of soil to become liquefiable. Thus, a liquefaction assessment method that takes the influence of the underground structure is adopted. The upheaval of underground structure caused by liquefaction should be checked when the base of the underground structure is within soil that is determined as liquefiable following the new liquefaction assessment method. The Chinese code for seismic design of underground structures is based on the accumulation of knowledge and experience in both practice and research over the past decades, and provides a framework for the seismic design of underground structures in China. As further findings and challenges arise in the future, new design methods and measures should be adopted and included in the code.

7. ACKNOWLEDGMENTS

The authors would like to thank the National Natural Science Foundation of China (No. 51678346 and No. 51708332) for funding the work presented in this paper.

8. REFERENCES

PRC National Standard (2010). Code for seismic design of buildings (GB 50011-2010), The Ministry of Housing and Urban-Rural Construction of the People's Republic of China, China Architecture & Building Press, Beijing, China.

Samata S, Ohuchi H, Matsuda T (1997). A study of the damage of subway structures during the 1995 Hanshin-Awaji earthquake. *Cement and concrete composites*, 19(3): 223-239.

Tokimatsu K, Tamura S, Suzuki H, Katsumata K (2012). Building damage associated with geotechnical problems in the 2011 Tohoku Pacific Earthquake. *Soils and Foundations*, 52(5):956-974.

Uenishi K, Sakurai S (2000). Characteristic of the vertical seismic waves associated with the 1995 Hyogo-ken Nanbu (Kobe), Japan earthquake estimated from the failure of the Daikai Underground Station. *Earthquake Engineering and Structural Dynamics*, 29(6): 813-822.

Wang R, Zhang J M, Wang G (2014). A unified plasticity model for large post-liquefaction shear deformation of sand. *Computers and Geotechnics*, 59:54-66.

Yasuda S, Harada K, Ishikawa K, Kanemaru Y (2012). Characteristics of liquefaction in Tokyo Bay area by the 2011 Great East Japan earthquake. *Soils and Foundations*, 52(5):793-810.

Yamaguchi A, Mori T, Kazama M, Yoshida N (2012). Liquefaction in Tohoku district during the 2011 off the Pacific Coast of Tohoku Earthquake. *Soils and Foundations*, 52(5):811-829.